



Validation of an optical sensor-based high-throughput bioreactor system for mammalian cell culture

Xudong Ge^a, Michael Hanson^{a,b}, Hong Shen^a, Yordan Kostov^a, Kurt A. Brorson^b, Douglas D. Frey^a, Antonio R. Moreira^a, Govind Rao^{a,*}

^a Center for Advanced Sensor Technology, Department of Chemical and Biochemical Engineering, University of Maryland, Baltimore County, 1000 Hilltop Circle, Baltimore, MD 21250, United States

^b Office of Biotechnology Products, Center for Drug Evaluation and Research, Food and Drug Administration, 8800 Rockville Pike, Bethesda, MD 20892, United States

Received 17 August 2005; received in revised form 27 October 2005; accepted 7 December 2005

Abstract

Cell culture optimization is a labor-intensive process requiring a large number of experiments to be conducted under varying conditions. Here we describe a high-throughput bioreactor system that allows 12 mini stirred-tank bioreactors to be operated simultaneously. All bioreactors are monitored by low-cost minimally invasive optical sensors for pH and dissolved oxygen. The sensors consist of single-use patches affixed inside the bioreactors and monitored optically from the outside. Experimental results show that different sensing patches with the same composition respond consistently. The discrepancy between different pH sensors is less than 0.1 pH units over most of their responsive range. The discrepancy between different dissolved oxygen sensors is less than 10% over the whole range from 0% to 100% dissolved oxygen. The consistency of the sensing system ensures that only an initial one-time calibration is required for the sensing patches. After that, a calibration code is generated and sensing patches of the same composition can be used directly. This greatly reduces the time and cost required for monitored multi-bioreactor operations. We used SP2/0 myeloma/mouse hybridoma cell cultures to demonstrate reactor performance consistency. Transcriptional profiling, HPLC analysis, viable cell count, and viability inspection show that the presence of sensing patches and the use of optical monitoring have no apparent effect on the metabolism of the cells.

© 2006 Elsevier B.V. All rights reserved.

Keywords: Optical sensor; Non-invasive; High-throughput bioreactor; Mammalian cell culture; Transcriptional profiling

1. Introduction

Although much progress has been made in the biotechnology industry, the development of bioprocesses is still rather labor-intensive and inefficient. In

* Corresponding author. Tel.: +1 410 455 3432; fax: +1 410 455 6500.

E-mail address: grao@umbc.edu (G. Rao).

order to bring a high quality product to the market as soon as possible, it is highly desirable to optimize the bioprocess expeditiously. Bioprocess optimization typically involves three major tasks: strain selection, media formulation, and selection of critical process parameters. Strain selection is to select the best producing colony from an early stage culture. Media formulation is developed to find the best combination of different nutrients such as sugars, amino acids, vitamins, minerals, and hormones. Because there are so many different nutrients, the combinational possibilities are enormous. Selection of critical process parameters is done to identify the ideal conditions and the allowable range for each variable. Some of the parameters are pH, dissolved oxygen (DO), feeding strategy, culture temperature, seeding cell density, induction time, and harvest time. In each of the above three tasks, a large number of experiments under varying conditions have to be conducted in order to determine the best colony or the optimal environmental and nutritional conditions.

The most commonly used devices for bioprocess optimization are laboratory-scale bioreactors and shake flasks. Laboratory-scale bioreactors equipped with various types of probes can provide more information about the bioprocesses than shake flasks. However, because experiments performed with laboratory-scale bioreactors are more labor-intensive and time-consuming, many compromises are often made during process optimization in order to keep the number of experiments down. Thus, there is a good chance that the optimal conditions may be missed. Even with compromises, process optimization could take more than a hundred runs, and often could last a year or more. Although process optimization performed in shake flasks is less labor-intensive and expensive, the conditions are generally not monitored, and only agitation and temperature are controlled. Thus, such studies can only provide limited information about the bioprocess.

To speed the process of new products going to the market, the development of fully instrumented high-throughput bioreactors that enable a large number of experiments in a short period of time is of great significance. Several companies and research groups are developing high-throughput bioprocessing devices for process optimization, and some are commercially available. Infors AG (Bottmingen/Basel, Switzerland) developed a Sixfors system, which is basically six laboratory-scale fermenters set side-by-side

on a large platform. The advantages of this system over six individual fermenters are in reactor uniformity and a unified control. DASGIP (Jülich, Germany) developed a parallel shake flask system modified to accept DO and pH electrodes for process control. These systems use industry standard sensors for process monitoring or control. As these probes are expensive and non-disposable, their cleaning, sterilization, and calibration between experiments are still relatively time-consuming. Weuster-Botz et al. developed a gas-inducing milliliter-scale bioreactor system with a maximum of 48 stirred-tank reactors arranged in a bioreaction block (Puskeiler et al., 2005; Weuster-Botz et al., 2005). DO concentration was monitored online with fluorometric sensor spots immobilized onto the reactor bottom. OD and pH were monitored by automatically taking samples into commercially available microtiter plates, which were then transported to a plate reader. Maharbiz et al. (2004) presented an array of eight 250 μ l microbioreactors each with closed-loop temperature control, adjustable oxygen supply generated electrochemically, and continuous pH and OD monitoring. Another approach to the development of high-throughput bioprocessing devices is the use of standard well plates supplemented with some type of sensing as microbioreactors (Girard et al., 2001; John et al., 2003; Lye et al., 2003). Measurements of process parameters were performed with commercial plate readers. Zanzotto et al. (2004, 2005) developed a membrane-aerated microbioreactor with only 5–50 μ l working volume using commercially available sensor foils for pH and DO monitoring. The microbioreactor was successfully used in gene expression analysis. Since mass transport at this scale is diffusive rather than convective as in larger-scale fermentors, it is unclear whether this will be a scalable approach. Mass transfer into microtiter places with a view to high-throughput bioprocessing applications has been characterized (Hermann et al., 2002). Bioprocessors (Woburn, MA) have recently introduced a system capable of several hundred simultaneous cultivations at the hundred microliter scale. Both these systems by virtue of a high surface to volume ratio are capable of high volumetric mass transfer coefficients.

In this paper, we report the validation of an optical sensor-based stirred-tank high-throughput bioreactor system. This system can hold twelve 30-ml bioreactors with the two most important parameters (pH and

DO) being monitored by disposable optical sensors. The advantages of stirred-tank bioreactors include their wide applications in bioprocessing and the existence of a vast body of previous experience in design and scale-up. Miniature stirred tanks using optical sensors have been analyzed for their suitability in high-throughput bioprocessing (Lamping et al., 2003; Harms et al., 2006). Optical sensors have the advantages of being non-invasive, easily miniaturized, and low cost (Ge et al., 2003, 2004; Harms et al., 2002; Kostov et al., 2001). As sensing patches with the sample composition have the same analyte response, only a one-time calibration of the entire sensor lot is necessary. This allows for far simpler operation in practice, as sensors need not be calibrated individually. In this paper, the reliability and consistency of the sensing system, which is the basis of so-called calibration-free sensing, were evaluated. The performance of the bioreactors was evaluated with SP2/0 myeloma/mouse hybridoma cell cultures, and the possible effect of the sensor patches and excitation light on the metabolism of cells was examined. Although this system was not equipped with control capabilities, it provides an important first validation of the effect of optical monitoring on cell growth and product formation.

2. Materials and methods

2.1. The high-throughput bioreactor (HTBR) system

The HTBR system is shown in Fig. 1. The system consists of 12 mini stirred-tank bioreactors equipped with disposable DO and pH optical sensing patches (only 1 bioreactor and its agitation motor are shown), a detector board, a gas distributor, a turntable and is a commercial product made by Fluorometrix (Stow, MA). The turntable is hollow and also serves as a water bath. The bioreactors are 30 mm in diameter and 78 mm in height with a working volume of approximately 30 ml (Fig. 2). All the bioreactors were positioned on a turntable, which was driven by a stepper motor underneath it. Agitation was provided by two 6 mm × 18 mm paddles powered by the agitation motors. Each bioreactor has a fluorescence-based pH patch and a DO patch on the bottom, allowing on-line measurement of the two most important process parameters (Kermis et al.,

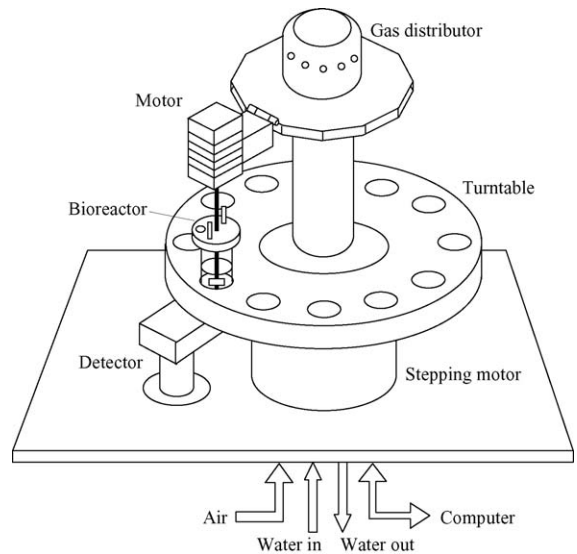


Fig. 1. High-throughput bioreactor (HTBR) system. The system can hold 12 stirred-tank bioreactors, but only one is shown here.

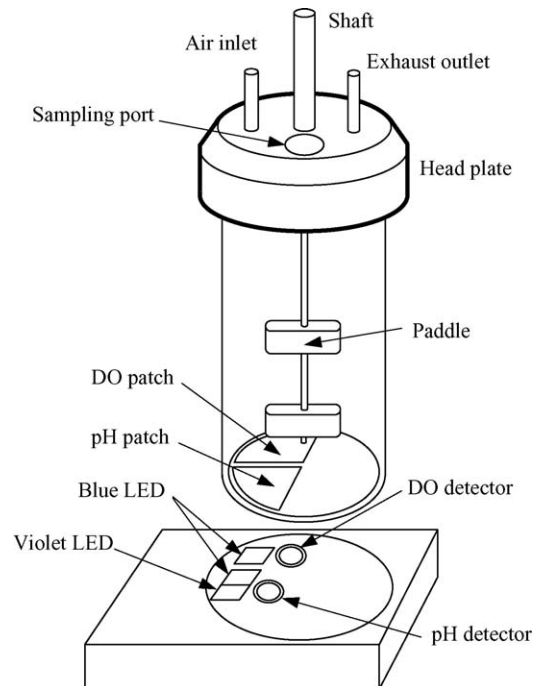


Fig. 2. The bioreactor and the monitoring system. Interference filters are positioned in front of the LEDs and photodiodes (not shown). Note that the sensing patches were affixed on the bottom while the LEDs and detectors were positioned outside. The advantage of this strategy is that the measurement is only partially invasive, but appropriate alignment of each patch to its corresponding optics is required.

2002, 2003; Tolosa et al., 2002). There are currently no closed-loop controls for pH and DO. This feature will be added to the next generation of the HBTR system. Temperature was controlled at 37 °C by circulating water between a refrigerated constant temperature circulator (Polyscience, Niles, IL) and the turntable. The inlet air, nitrogen and carbon dioxide were supplied from laboratory air supply, N₂ and CO₂ cylinders, respectively. Gas mixtures were obtained by blending different gases through two flowmeters (FM4332 and FM4333, Advanced Specialty Gas Equipment Corp., South Plainfield, NJ). The gas mixture thus obtained was sent to the gas distributor, which consists of a single inlet chamber with 12 outlets. Individual bioreactors connect to each outlet through plastic or rubber tubing followed by a 0.2- μ m filter, and then to a sparger that delivers air into the media. There is currently no ability to individually meter air flow into each reactor.

The system was controlled by a computer equipped with a LabJack U12 card (LabJack Co., Lakewood, CO) using a custom LabVIEW program. Agitation speed could be adjusted continuously from 10 rpm to 1000 rpm in each bioreactor. Process parameters in one bioreactor were measured one at a time. After all the process parameters for one bioreactor were measured, the turntable rotated the next bioreactor above the detector. One measurement cycle takes from approximately 20 s to 4 min, depending on how many bioreactors are monitored.

For the present, only the optical sensing patches were made of disposable materials. The vessels were made of glass and the headplates were made of stainless steel. The current reactor is designed such that the glass vial with patches can be discarded after a single use. In the future, the reaction vessels and the accessories will be molded from biologically compatible disposable materials. Thus, the entire bioreactor including the optical sensing patches will be completely disposable. This development will significantly decrease the time and labor involved in performing experiments.

2.2. DO and pH monitoring

The oxygen sensor patches used in this study were provided by Lumet LLC (Bethesda, MD). The Lumet patches have three different layers: a responsive layer, an adhesive layer, and a white backing layer. The

responsive layer is a layer of silicone rubber with an oxygen-responsive fluorophore immobilized in it (Tolosa et al., 2002). The adhesive layer is used for attaching to the bottom of the bioreactor. The white backing layer is designed to prevent autofluorescence from the growth media from affecting the fluorescence measurements.

The fluorophore immobilized in the DO patches is a long-lifetime fluorophore (Kostov et al., 2000b,c; Tolosa et al., 2002; Van Houten et al., 1998). When the fluorophore is excited by an intensity-modulated light source, the intensity of the resulting emission appears at the same frequency but with lower modulation and a phase shift. Because the fluorescence of the fluorophore is quenched in the presence of oxygen, the phase shift will change in response to a change in DO concentration.

The instrumentation to measure the phase shift uses a blue LED (Sharp Electronics Corp.) with a shortpass filter (Schott, Germany), and a PIN photodiode (BPW32, Vishay, France) with a longpass filter (Andover Corporation, NH). The LED was driven with a simple transistor driver that was controlled by the reference of an in-house built lock-in amplifier and modulated at 10 kHz. The photodetector output was connected to the signal input of the lock-in, and phase was measured (Harms et al., 1999).

The calibration of the DO patches was done in PBS buffers (pH 7.2). Six bioreactors with DO sensing patches were used for the calibration. The bioreactors were each added 20 ml of PBS buffer, and then placed on the turntable at positions 1, 3, 5, 7, 9, and 11, respectively. The gas mixture with desired O₂ content was obtained by mixing air and nitrogen whose flow rates were adjusted by flowmeters. The gas mixture bubbled through the PBS buffer. The temperature was maintained at 37 °C all the time.

The pH sensor patches used in this study were developed by the authors' laboratory (Kermis et al., 2002, 2003). They also have three different layers: an adhesive layer, a responsive layer, and a support layer. The adhesive layer has the same functions as the DO patches. The responsive layer is a hydrogel-white backing composite layer with the sensing fluorophore 6,8-dihydroxypyrene-1,3-disulfonic acid disodium salt (DHPDS) covalently immobilized in it. The white backing serves as both a support for the hydrogel and an optical isolator from the autofluorescence from the

media. Because the mechanical strength of the hydrogel is weak, an additional support layer (polyester film) was added between the adhesive layer and the responsive layer to enhance the patch's mechanical strength. Because of the high stability of the dye, the pH sensing patches can last 2 months with little drift.

The responsive fluorophore (DHPDS) immobilized in the pH patches possesses two excitation maxima at wavelength of 405 nm and 465 nm, corresponding to the protonated and deprotonated forms of the fluorophore. As a change in pH breaks the dissociation equilibrium of the fluorophore, the amount of the fluorophore in one of the two forms will increase while the other will decrease until a new equilibrium is reached. Correspondingly, the ratio of the two excitation maxima (R) will change.

The two excitation sources for the pH patches were a blue LED and a violet LED with a shortpass filter. The emission was filtered by a bandpass filter (Intor Inc., Socorro, NM) before reaching a PIN photodiode. The photocurrent was amplified by a transimpedance stage and a simple lock-in amplifier, both of which were developed in-house (Kostov et al., 2000a).

The pH sensors were calibrated using PBS or bicarbonate buffers of known pH and a constant ionic strength of 0.15 M with phosphate or carbonate buffering species at 73 mM and sodium chloride added to achieve the desired ionic strength. The pH of the buffers was verified with an AR25 Dual Channel pH/Ion Meter (Fisher Scientific, Pittsburgh, PA) before calibration. The temperature was also maintained at 37 °C all the time.

2.3. Cell culture

A SP2/0 based myeloma/mouse hybridoma cell line (2055.5) secreting an IgG3 antibody specific for the *Neisseria meningitidis* capsular-polysaccharide (MCPS) (Rubinstein and Stein, 1988) was maintained in a 250-ml spinner flask (Kontes, Vineland, NJ) in CD Hybridoma protein-free media (Gibco Brand, Carlsbad, CA) supplemented with 2 mM glutamine (HyClone, Laboratories Inc., Logan, UT), 100 U/ml penicillin (HyClone), 100 µg/ml streptomycin (HyClone), 1 g/l PF-68 (MP Biomedicals, LLC, Aurora, OH), and 3.5 × 10⁻⁴% β-mercaptoethanol (v/v) (Sigma, St. Louis, MO, USA). The flask was kept in a water-jacketed incubator (Napco, Winchester, VA)

at 37 °C and 50% relative humidity with a headspace CO₂ composition of 5% in air.

Before performing the cell cultures on the HTBR, the air inlets and outlets of all vessels were covered with 0.22 µm syringe filters (Millex-GV, Millipore, Bedford, MA, USA). All vessels were then steam sterilized at 121 °C for 25 min. Upon cooling, each vessel was first rinsed with media and then filled with 35 ml of cell culture media inoculated with 0.1 × 10⁶ cells/ml of media in a laminar flow hood. To explore the effect of patches and excitation lights (460 nm and 405 nm) on cell growth and culture environment, the experiment was carried out with cells being grown in three different situations. Among the 11 vessels used, vessels 1–5 had sensing patches and were monitored [patch(+)/light(+)], vessels 7–9 had no patches and were not monitored [patch(-)/light(-)], vessels 10–12 had no patches but were illuminated with excitation light like the monitored vessels [patch(-)/light(+)]. Vessel 6 was not used. The temperature and agitation speed was controlled at 37 °C and 300 rpm in all vessels. The vessel headspace was open to the atmosphere via 0.22 µm syringe filters. All light(+) vessels were illuminated every 30 min for monitoring or comparison. Samples were taken once a day with syringes through the sampling port on the vessels. Cells in the samples were counted using a hemocytometer, and viability was determined using the trypan blue exclusion method. At 45 h, 5 ml of culture were withdrawn from each of the bioreactors for transcriptional profiling. Final culture supernatants from the 11 reactors were analyzed using a high-throughput size-exclusion chromatography system.

Although the bioreactors were equipped with air spargers for culture aeration, it was found to be difficult to realize uniform air distribution among the bioreactors since individual needle valves were not employed for each reactor. This has also been previously observed in our prior work (Harms et al., 2006). As the main goal of the present study was to check the consistency and repeatability of the sensing system, and its effects on the cells, other factors affecting the growth of the cells such as non-uniform air distribution were deliberately avoided. Thus, no aeration other than by diffusion through the inlet and outlet filters was provided in the cell culture. Further studies using homogeneous air distribution among bioreactors are being conducted.

2.4. Transcriptional profiling

2.4.1. RNA extraction, reverse transcription, and DNA microarray hybridization

Total RNA from monitored [patches(+)/lights(+)] and control [patches(-)/lights(-)] cultures was extracted with Trizol (Gibco Brand) and chloroform (Mallinckrodt, Phillipsburg, NJ) and purified using the RNeasy Mini-Prep kit (Qiagen Inc., Valencia, CA). An indirect experimental design utilizing common reference RNA was used in the microarray study. For each DNA microarray, the following procedure was carried out. mRNA in 20 µg of total RNA [from cultured cells or a murine reference pool (Becton, Dickinson, and Co., Franklin Lakes, NJ)] was primed with 0.05 µg/µl oligo-dT²⁰ (FDA/CBER Core Facility, Bethesda, MD) on ice for 10 min following a 10 min incubation at 70 °C. Primed mRNA was reverse transcribed to cDNA with 0.02–0.05 mM dNTPs (Invitrogen, Carlsbad, CA) and 3.33 U/µl reverse transcriptase (Stratagene, La Jolla, CA) in 1× first strand buffer (Stratagene) with 0.01 M DTT (Sigma) in a reaction at 42 °C lasting for 90 min. Non-reverse transcribed RNA and excess reaction reagents were removed using a MinElute PCR Purification Kit (Qiagen). The purified cDNA was fluorescently labeled with either Cy3 (reference cDNA) or Cy5 (culture cDNA) dyes (Amersham, Piscataway, NJ) for 90 min in 0.1 M NaHCO₃ (pH 9) coupling buffer (Sigma). Residual dye was removed afterwards with the same PCR Purification Kit.

Microarrays (16,896 spots, including positive/negative controls, and genes, some multi-spotted) obtained from the NCI/CBER microarray facility were pre-hybridized with 5× SSC buffer (American Bioanalytical, Natick, MA), 1% BSA (w/v) (Sigma), and 0.1% SDS (w/v) (Sigma) for 1 h, washed in DEPC-treated H₂O (MP Biomedicals, Irvine, CA) and isopropanol (American Bioanalytical) and spin-dried at 100 × g for 5 min in a table top centrifuge (Beckman, Fullerton, CA). Purified labeled cDNA from a single reactor was mixed with purified labeled cDNA from the reference pool and 32 µl of hybridization buffer (Ambion, Austin, TX), forming the hybridization solution, which was stored in the dark at 42 °C until usage. Immediately prior to hybridization, MAUI hybridization mixers (Biomicro, Salt Lake City, UT) were affixed to the microarray slide surfaces. Hybridization solution was injected into the mixers and the microarrays were

placed into the MAUI hybridization chamber (Biomicro) for hybridization overnight at 42 °C.

2.4.2. Scanning, image processing, and data analysis

The microarrays were washed with 1× SSC (0.05% SDS) and 0.1× SSC, each for 4 min, and scanned for Cy3 and Cy5 signal intensities using a GenePix 400B microarray scanner (Axon, Union City, CA). Image processing (automatic and manual spot selection/rejection) was carried out using GenePix Pro 6.0 (Axon).

Using BRB ArrayTools software (<http://linus.nci.nih.gov/BRB-ArrayTools.html>, National Cancer Institute, Bethesda, MD), genes on individual arrays were filtered out according to their background subtracted fluorescence intensities. Ratios of the Cy5 and Cy3 signals were log-transformed and then normalized with a Lowess smoother, which takes into consideration dye intensity biases (Yang et al., 2002). Microarrays were carried out for four monitored and three control reactors. ArrayTools was then used to compare gene expression in the two groups of arrays by carrying out a Class Comparison analysis. The analysis utilizes a random-variance *t*-test (Wright and Simon, 2003) to identify genes that are differentially expressed (*p*-value <0.001) as a result of a change in culture conditions which, in this case, is the presence of the HTBR sensing system (DO and pH patches and excitation lights of varying wavelengths).

2.5. Size-exclusion chromatography

The size-exclusion chromatographic experiments were performed on an Ultimate HPLC instrument coupled to a FAMOS autosampler (LC Packings—Dionex, Sunnyvale, CA, USA) and controlled by Chromeleon software Version 6.6 (Dionex). The columns used were a 3.5 cm × 0.46 cm (i.d.) Super SW guard column and a 30 cm × 0.46 cm (i.d.) TSK-GEL Super SW3000 separation column placed in series (TosohBioscience, Montgomeryville, PA, USA). The samples from the micro-bioreactors were filtered through 0.2 µm polysulfone filters (Millipore) and stored in a 96 deep well plate in the FAMOS with the cooling system adjusted to 8 °C. A 100-µl sample loop was used for sample injection, and a conventional UZ-view flow cell with a 10 µl volume was used for UV detection.

The flow rate in the experiments was controlled at 0.1 ml/min, and the column effluent was monitored at both 260 nm and 280 nm. The eluent buffer was composed of 100 mM sodium phosphate and 300 mM sodium chloride (Sigma) at pH 7, and was degassed by vacuum filtering using a 47 mm diameter nylon membrane filter with 0.2 μ m pores (Whatman, Clifton, NJ, USA).

3. Results and discussion

3.1. Mechanical stability

For a high-throughput bioreactor system, the most important feature is the parallel operation of process monitored bioreactors. To produce meaningful results, the sensing system of the parallel bioreactors must behave consistently, and all bioreactors must have comparable performance under the same conditions. This is especially important for the high-throughput bioreactor system described here, as the ultimate goal of our present study is a completely disposable system with calibration-free sensing capability. As long as the sensing system and the performance of the bioreactors are reliable and repeatable, other actions like closed-loop control, nutrient feeding, etc. can be performed with little difficulty. While the above comments apply to any bioreactor equipped with conventional DO and pH sensors, another very important question must be answered for optically monitored bioreactors. It is important to demonstrate that the blue and violet light used for sensor excitation has no measurable effect on the growth of the cells, their gene expression and the product quality. Because the success of the HTBR system and of optical monitoring in general is greatly dependent on these features, a major part of this work was devoted to the clarification and validation of these two aspects (i.e. consistency of operation and non-interference of the optical sensors).

The mechanical performance of the system was first evaluated by running the system continuously for several days. The temperatures inside different bioreactors were identical and no appreciable fluctuations were observed. The shafts of the agitators wobbled a little but their speeds were even, and the transition was smooth when the speed was adjusted from 10 rpm to 1000 rpm. The slight wobble of the shafts could be overcome by

improving the bearing structure and the manufacturing precision.

3.2. Reliability and repeatability of the sensing system

To check the reliability and repeatability of the sensing system, six vessels with DO and pH sensing patches were used. The responsive layer of the DO sensing patches is a layer of silicone rubber with an oxygen-responsive fluorophore immobilized in it. For a single-emitting fluorophore, the phase shift (N) of the resulting emission when excited by an intensity-modulated light source applies (Lakowicz, 1999; Tolosa et al., 2002),

$$\frac{\tan(N_0)}{\tan(N)} - 1 = K_{SV}[Q] \quad (1)$$

where N_0 is phase shift of the fluorophore in the absence of the quencher, K_{SV} is the Stern Volmer constant, and $[Q]$ is the concentration of the quencher. However, because there are dual-emitting species (Kostov et al., 2000b,c), the fluorophore in the DO patches does not completely follow the above linear equation. Here we used a non-linear equation to fit the DO calibration data,

$$P = \frac{\tan(N_0)}{\tan(N)} - 1 \quad (2)$$

$$[O_2] (\%) = AP^2 + BP \quad (3)$$

where $[O_2]$ is the DO concentration, A and B are constants shown in Fig. 3.

The calibration data and the fitted curve are shown in Fig. 3. It can be seen that a second-order polynomial fits the calibration data very well. The accuracy and consistency of the sensors is shown in Fig. 4. It can be seen that the six different DO patches gave consistent results with an average relative error of 9.0% from the real values. The fluctuation of the DO readings at 48.5% and 100.0% was caused by the instability of the flowmeters. To check if the cell culture media affect the calibration, the DO readings in PBS buffer and in cell culture media were compared at several different DO concentrations. The DO readings in PBS buffer were $0.1 \pm 0.1\%$, $9.8 \pm 0.3\%$, $25.0 \pm 0.6\%$, $27.8 \pm 0.4\%$, and $100.1 \pm 3.4\%$ while in cell culture media they were $0.0 \pm 0.0\%$, $9.4 \pm 0.1\%$, $24.6 \pm 0.4\%$, $27.7 \pm 0.5\%$, and $99.8 \pm 10.2\%$. Statistical analysis

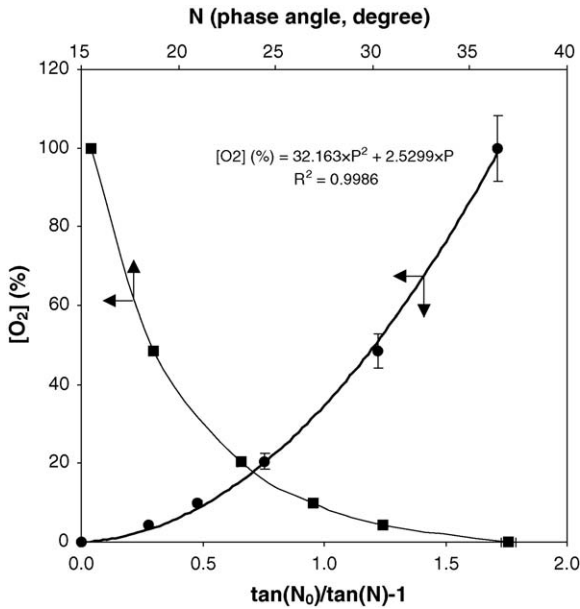


Fig. 3. Calibration of the dissolved oxygen patches. Calibration was done in PBS at 37 °C using six vessels each with a DO sensing patch. Gas mixtures of known composition were passed through each vessel. The error bars shown in the figure stand for the standard deviation of the six different readings, which are 0.4%, 0.8%, 2.0%, 4.4%, and 8.3% at DO concentrations from 4.3% to 100.0%. Divided by the corresponding DO concentrations, these deviations gave an average relative error of 9.0% from the real values.

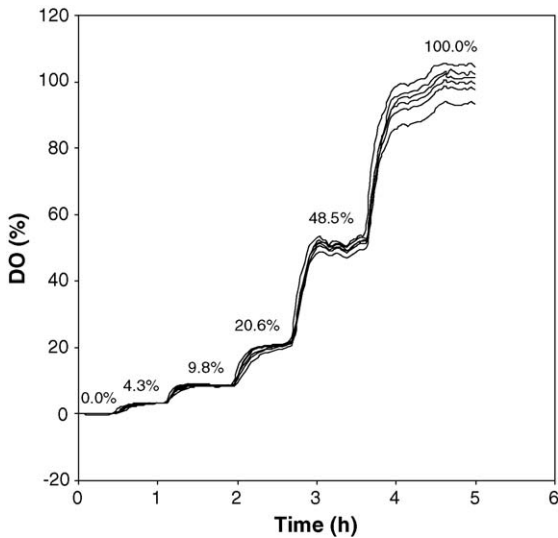


Fig. 4. Consistency of DO measurements in six different vessels.

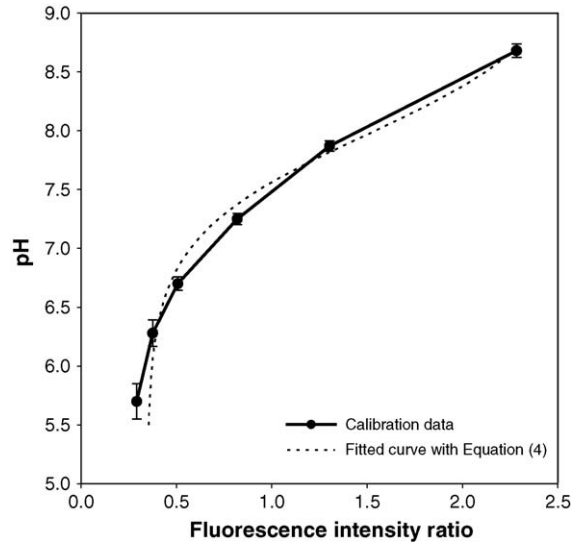


Fig. 5. Calibration of the pH patches. Calibration was done in PBS or bicarbonate buffers of known pH at a constant ionic strength of 0.15 M at 37 °C using six vessels each with a pH sensing patch. The error bars stand for the standard deviation of the six different readings, which are 0.15, 0.11, 0.06, 0.05, 0.05, and 0.06 pH units, respectively, from pH 5.70 to 8.68.

showed that there was no significant difference between the two sets of readings. The average 90% response time of the DO sensors is 12.6 min from air to nitrogen, and 10.8 min from nitrogen to air. Although not very rapid, these response times are more than sufficient for monitoring the slow DO changes typical of cell cultures.

The calibration data of the pH patches is shown in Fig. 5. The error bars represent the average deviations of the readings of the six sensors. For this kind of pH sensor, the following equation is often used to fit the calibration data (Kermis et al., 2003):

$$R = \frac{[H^+]R_{min} + K_{app}R_{max}}{[H^+] + K_{app}} \tag{4}$$

where R_{max} and R_{min} are the ratios of the two excitation maxima (460 nm/405 nm) for the deprotonated and protonated forms of the fluorophore, respectively, $[H^+]$ is the molar concentration of the hydrogen ions, and K_{app} is the apparent association constant of the fluorophore. The fitted line for Eq. (4) is shown in Fig. 5 (the dotted line). It can be seen that although it is more convenient to use, this equation can introduce big errors

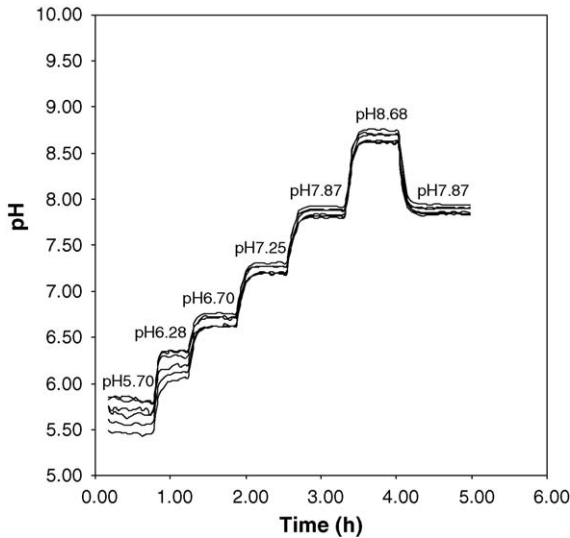


Fig. 6. Consistency of pH measurements in different vessels.

under pH 6.0. To avoid this problem, the pH values were calculated by linear interpolation.

The consistency of the sensors is shown in Fig. 6. It can be seen that all six sensors gave very similar results at pH above 6.5. At pH below 6.0, the sensitivity of the sensors is lower, and the consistency of the sensors decreases because a small error in intensity measurement can cause a relatively large error in pH. The average deviation of the sensors is 0.15, 0.11, 0.06, 0.05, 0.05, and 0.06 pH units, respectively, from pH 5.70 to 8.68. The maximum deviation is 0.23, 0.16, 0.07, 0.06, 0.06, and 0.07 pH units, respectively. Variance analysis showed that no significant difference existed between the 12 different positions on the turntable at 95% confidence level. Thus, the reasons for this discrepancy are limited to the patches and the bioreactors. Factors that may affect the consistency of the readings of different sensors include the uniformity of the patches, the size and alignment of the patches, the shape of the bioreactor bottoms, etc. Although the consistency of the readings is already quite good especially at pH above 6.5, it can be further improved by optimizing these factors. The average 90% response time is 5.4 min from pH 6.28 to 7.87, and 2.4 min from pH 7.87 to 6.28, which is rapid enough for cell culture monitoring. To confirm that the calibration done in PBS is applicable to cell culture, the pH of the fresh media was measured with the HTBR and the AR25

Dual Channel pH/Ion Meter. The two devices showed similar results, which were 8.8 ± 0.1 for the HTBR and 8.90 for the pH meter.

From the results shown above, it can be seen that different sensing patches with the same composition responded consistently. This is of great significance because it implies that the sensing patches need to be calibrated only once. After that, a calibration code is generated and the sensing patches with the same composition can be used directly for the next culture with no need for recalibration. Unlike optical probes in which the relative positions of the components are fixed, the detectors and the sensing patches used in this study were separate (Fig. 2). The advantage of this strategy is that the measurement is only partially invasive. Because the patches are autoclavable, they can be steam sterilized with the bioreactors. There is no direct contact between the external instrumentation and the culture during the process. This greatly reduces the chance of contamination. However, as the two components are separate, the alignment of the two is important. To obtain repeatable results, the sensing patches need to be positioned at the same positions right above the detector board (Fig. 2).

3.3. Performance consistency of bioreactors

To check the consistency of bioreactor's performance and the effect of the excitation light on the cell growth, cell cultures experiments were conducted in the system. The batch cell cultures lasted approximately 70 h. Samples were taken once a day for cell count and viability inspection. During the microscopic (400 \times) inspection of the samples, no visually detectable contamination was found in any of the 11 vessels during the cell culture.

Fig. 7 shows the DO and pH profiles in the five monitored vessels during the cell cultures. It can be seen that the cultures in all five bioreactors behaved almost identically. All DO and pH profiles followed the same trend, with only a 2.7% average difference in DO concentration, and a 0.09 unit average difference in pH. The oxygen levels were all continuously decreasing with time until totally depleted at approximately 40 h. The oxygen-limiting conditions persisted for 5 h. At 45 h, 5 ml of culture was withdrawn from each of the five bioreactors for transcriptional profiling. The withdrawal of 5 ml of culture sucked the same volume of

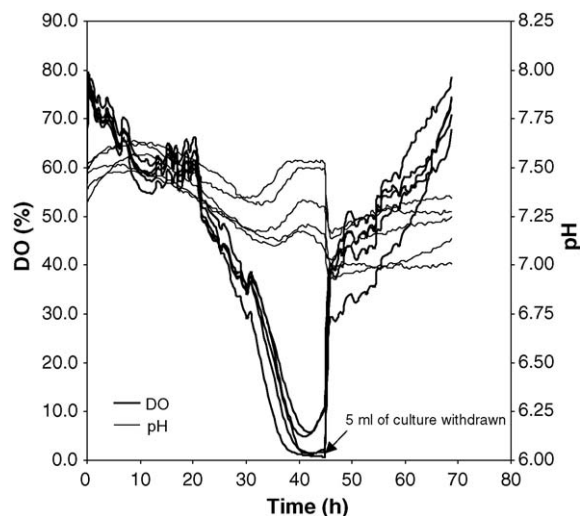


Fig. 7. DO and pH profiles in myeloma/mouse hybridoma cell cultures.

air into the bioreactor, increasing the oxygen concentration in the headspace abruptly. This abrupt increase again induced an abrupt increase in DO concentration in the media. The subsequent gradual increase in DO concentration was caused by the lowered oxygen consumption as more and more cells began to die in the decline phase due to the depletion of energy or nutrient source. The pH increase during the first 10 h was likely caused by the gradual release of the CO₂ from the media, which was previously in equilibrium with 5% CO₂ when kept in the incubator. The culture became increasingly more acidic in the subsequent 20 h because the cells produced increasing amount of CO₂ as they grew. At the last stage of the exponential growth phase, the production of CO₂ by the cells slowed down, and pH began to increase again. The abrupt decrease in pH after the 5 ml of culture was withdrawn was probably caused by the escape of ammonia from the media. As the major nutrient and energy source for mammalian cell culture, glutamine could be metabolized through several different pathways, resulting in different energy output and ammonia release (Genzel et al., 2005). The ammonia thus formed likely accumulated in the medium and in the headspace above the media. The introduction of fresh air due to the sample withdrawal diluted the ammonia concentration in the headspace, causing the release of ammonia from the media. We are designing experiments to verify this observation definitively.

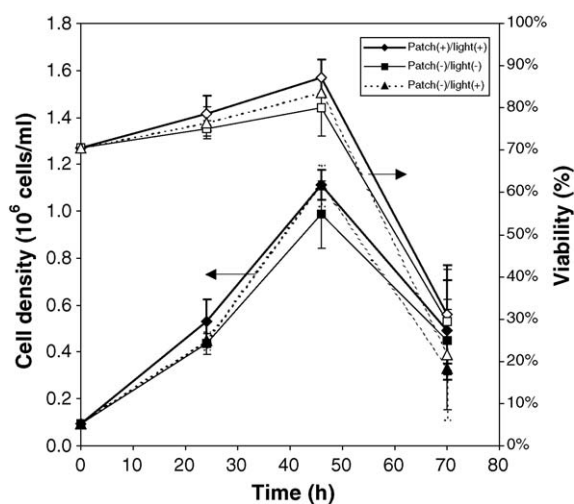


Fig. 8. Cell density profiles and viability profile in monitored and control myeloma/mouse hybridoma cell cultures.

As the sensing patches were in contact with the cultures, and the patches were illuminated with excitation light once every 30 min, it was important to check if they have an effect on the cell growth. Fig. 8 shows the viable cell densities in cultures growing under three different conditions ([patch(+)/light(+)], [patch(-)/light(-)], and [patch(-)/light(+)]) and the viabilities of the cells. It can be seen that the viable cell densities and the viabilities of the cells in the three different situations are quite similar. *F*-test and Student's *t*-test showed that there was no significant difference between the three groups of data. The viable cell densities and the viabilities of the cells in three different situations all reached maximum at 46 h, consistent with the DO profiles. After that, cell lysis dominated in the process, the viable cell densities and the viabilities of the cells both began to decrease.

3.4. DNA microarray analysis

DNA microarrays are a powerful technique to simultaneously monitor the activity of a large percentage of the cell transcriptome. Thus, it is exquisitely sensitive to changes in the cell culture state and can be used to definitively demonstrate culture consistency. DNA microarray analysis showed nearly identical gene expression profiles between cultures with and without monitoring. For example, in Fig. 9, the same portion of two different arrays is shown. One array

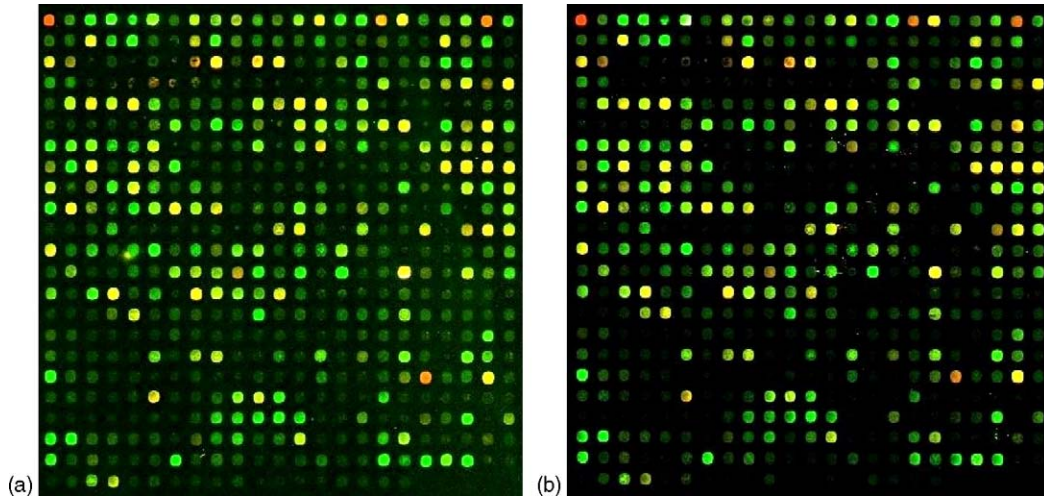


Fig. 9. The same portion from two different arrays, one from a control culture (a) and the other from a monitored culture (b). Red spots are indicative that the reactor cDNA present there is more abundant than the reference cDNA. Green spots designate the opposite. Yellow spots mean that the cDNA levels between the reactor and the reference pool are about equal. (For interpretation of the references to color in this figure legend, the reader is referred to the web version of the article.)

is from a monitored culture and the other is from a control. As can be seen, in that portion of the arrays the two samples show great similarity.

The similarity in the two expression profiles can also be seen by plotting the average logarithmic ratio of fluorescent signals $[\log_i(\text{Cy5}/\text{Cy3})]$ for each gene in the monitored cultures versus the average ratio in the control cultures, as in Fig. 10. In this plot, if the expression of a gene is the same in both situations, the data point should fall along the middle diagonal line, also known as the identity line, or $y=x$. The two lines in the plot above and below the identity line represent thresholds for two-fold differential expression. For this experiment less than 1% of the genes in the analysis (14,005 genes passed the signal intensity filter) exhibited an average differential expression of two-fold or greater. However, using the average expression value across a series of experimental replicates does not take into consideration important statistical aspects, such as the number of samples and the variability within the groups.

Conversely, the Class Comparison analysis in ArrayTools does take these and other statistically relevant pieces of information into consideration when determining if genes are differentially expressed. To do so, it uses a random-variance t -test, which is an improvement over the standard separate t -test as it per-

mits sharing information among genes about within-class variation without assuming that all genes have the same variance (Wright and Simon, 2003). Genes were considered statistically significant if their p -value

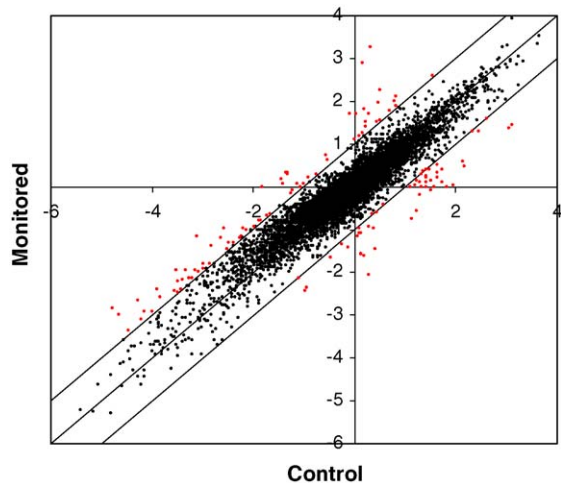


Fig. 10. A scatterplot of the average logarithmic ratio of fluorescent signals $[\log_i(\text{Cy5}/\text{Cy3})]$ of each gene in the monitored reactors vs. the average in the control reactors. Red spots are genes whose average expression is two-fold up or down. Total of 14,005 genes in the analysis, 128 of which are red. (For interpretation of the references to color in this figure legend, the reader is referred to the web version of the article.)

was less than 0.001. A stringent significance threshold was used to limit the number of false positive findings. This is necessary in the situation present here where with the number of genes, one would expect as many as 14 false positives. Here the Class Comparison analysis returned no statistically significant differentially expressed genes, further supporting the conclusion that the sensing instrumentation does not impact the cellular physiology of the cultures.

3.5. Size-exclusion chromatography

Final culture supernatants from the 11 reactors were analyzed using a high-throughput size-exclusion chromatography system. The chromatograms of the 11 reactors were compared to the chromatogram (data not shown) of the sterile media itself. Shown in Fig. 11 is the portion of the reactor chromatograms that is unique to the cell culture, i.e. none of peaks shown were present in the media chromatogram. Fig. 11 shows a variety of peaks spanning a retention time from 20 min to 45 min. As the detector is measuring the absorbance at 280 nm, the identities of the different peaks could be a wide variety of proteins, such as cellular products and metabolites, or nucleic acid. Regardless of the peak identities, it is obvious from the similarity in trends that the cell culture environment was nearly identical in all 11 reactors.

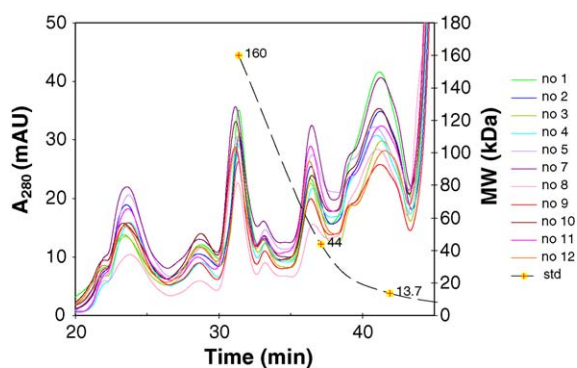


Fig. 11. A plot of a portion (retention time = 20–45 min) of the 11 reactor final supernatant size-exclusion chromatograms (reactor #6 not used) showing the absorbance at 280 nm (left axis). Three standard proteins: mouse IgG, ovalbumin, and RNase with molecular weights (right axis) of 160 kDa, 44 kDa, and 13.7 kDa, respectively, are plotted at their respective retention times. Reactors 1–5 [patches(+)/lights(+)], 7–9 [patches(-)/lights(-)], and 10–12 [patches(-)/lights(+)].

Table 1

The size-exclusion chromatographic retention times and final antibody titers of the 11 reactors

Configuration	Reactor no.	Retention time (min)	Antibody titer (mg/l)
Patch(+)/light(+)	1	31.38	94
	2	31.39	84
	3	31.43	80
	4	31.39	84
	5	31.26	92
		31.37 ± 0.06 ^a	87 ± 6 ^a
Patch(-)/light(-)	7	31.14	109
	8	31.29	75
	9	31.33	77
		31.25 ± 0.10 ^a	87 ± 19 ^a
Patch(-)/light(+)	10	31.18	109
	11	31.09	90
	12	31.14	86
		31.14 ± 0.04 ^a	95 ± 12 ^a
		31.27 ± 0.12 ^b	89 ± 11 ^b

Average = mean ± standard deviation.

^a Average.

^b Total average.

By using a mouse IgG standard (Southern Biotech, Birmingham, AL), the peak at the retention time of ~31 min was identified as our anti-MCPS IgG₃ product peak. The product peaks for each reactor were integrated and the areas were compared to the standard area to determine the final antibody titer in each reactor. The retention time for each product peak was measured as well. The results are summarized in Table 1. Statistical analysis shows that the retention time has no significant difference between the monitored [patches(+)/lights(+)] and the control [patches(-)/lights(-)], and there is also no significant difference between the light only group [patches(-)/lights(+)] and the control [patches(-)/lights(-)]. Based on the limited variation in retention time, no observable aggregation or fragmentation of the product is suspected. Also it appears that the sensing system has no inhibitory effect on the organism's total IgG₃ production capability.

4. Conclusion

This paper described a disposable optical sensor-based high-throughput bioreactor system for bioprocess development and optimization. All bioreactors

were monitored by low-cost disposable optical sensors for pH and dissolved oxygen. Results showed that all sensors in different bioreactors behaved consistently, and all bioreactors had similar performance under the same conditions. The discrepancy between different pH sensors was less than 0.1 pH units in most of their responsive range. The discrepancy between different dissolved oxygen sensors was less than 10% in the whole range from 0% dissolved oxygen to 100%. Because the sensors behave consistently, only a one-time initial calibration was required. After that, the sensing patches with the same composition could be used directly without need for further calibration. SP2/0 myeloma/mouse hybridoma cell cultures grown in the bioreactors exhibited consistent reactor performance. Transcriptional profiling and HPLC analysis showed that the sensing patches and the optical sensing system had no apparent deleterious effects on cellular physiology at the transcript level and on product quality.

Acknowledgements

This work was sponsored by NSF Grant BES0091705 and unrestricted funding from Merck & Co. The technology described in this paper has been licensed to Fluorometrix, in which some of the authors (X.G., Y.K., and G.R.) have an equity position. We thank Ruth Cordoba-Rodriguez for a careful review of this manuscript. Microarray analyses were performed using BRB ArrayTools developed by Dr. Richard Simon and Amy Peng. Views expressed in this article are those of the authors and not necessarily those of the US FDA or the US Government. Discussion of individual cell culture devices does not constitute an endorsement by the US FDA or US Government. Michael Hanson is partially funded by a PDA Pre-Doctoral Fellowship.

References

- Ge, X., Kostov, Y., Rao, G., 2003. High-stability non-invasive auto-clavable naked optical CO₂ sensor. *Biosens. Bioelectron.* 18, 857–865.
- Ge, X., Kostov, Y., Rao, G., 2004. Low-cost noninvasive optical CO₂ sensing system for fermentation and cell culture. *Biotechnol. Bioeng.* 89 (3), 329–334.
- Genzel, Y., Ritter, J.B., Konig, S., Alt, R., Reichl, U., 2005. Substitution of glutamine by pyruvate to reduce ammonia formation and growth inhibition of mammalian cells. *Biotechnol. Prog.* 21 (1), 58–69.
- Girard, P., Jordan, M., Tsao, M., Wurm, F.M., 2001. Small-scale bioreactor system for process development and optimisation. *Biochem. Eng. J.* 7, 117–119.
- Harms, P., Kostov, Y., Rao, G., 2002. Bioprocess monitoring. *Curr. Opin. Biotechnol.* 3, 124–127.
- Harms, P., Sipior, J., Ram, N., Carter, G.M., Rao, G., 1999. Low-cost phase-modulation measurements of nanosecond fluorescence lifetimes using a lock-in amplifier. *Rev. Sci. Instrum.* 70, 1535–1539.
- Harms, P., Kostov, Y., French, J.A., Soliman, M., Anjanappa, M., Ram, A., Rao, G., 2006. Design and performance of a 24 station high throughput microbioreactor. *Biotechnol. Bioeng.* 93 (1), 6–13.
- Hermann, R., Lehmann, M., Büchs, J., 2002. Characterization of gas-liquid mass transfer phenomena in microtiter plates. *Biotechnol. Bioeng.* 81, 178–186.
- John, G.T., Klimant, I., Wittman, C., Heinze, E., 2003. Integrated optical sensing of dissolved oxygen in microtiter plates: a novel tool for microbial cultivation. *Biotechnol. Bioeng.* 81, 829–836.
- Kermis, H.R., Kostov, Y., Harms, P., Rao, G., 2002. Dual excitation ratiometric fluorescent pH sensor for noninvasive bioprocess monitoring: development and application. *Biotechnol. Prog.* 18, 1047–1053.
- Kermis, H.R., Kostov, Y., Rao, G., 2003. Rapid method for the preparation of a robust optical pH sensor. *Analyst* 128, 1181–1186.
- Kostov, Y., Albano, C.R., Rao, G., 2000a. All solid-state GFP sensor. *Biotechnol. Bioeng.* 70, 473–477.
- Kostov, Y., Harms, P., Pilato, R.S., Rao, G., 2000b. Ratiometric oxygen sensing: detection of dual-emission ratio through a single emission filter. *Analyst* 125, 1175–1178.
- Kostov, Y., Van Houten, K.A., Harms, P., Pilato, R.S., Rao, G., 2000c. Unique oxygen analyzer combining a dual emission probe and a low-cost solid-state ratiometric fluorometer. *Appl. Spectrosc.* 54, 864–868.
- Kostov, Y., Harms, P., Randers-Eichhorn, L., Rao, G., 2001. Low-cost microbioreactor for high-throughput bioprocessing. *Biotechnol. Bioeng.* 72, 346–352.
- Lakowicz, J.R., 1999. *Principles of Fluorescence Spectroscopy*, second ed. Kluwer Academic/Plenum Publishers, New York.
- Lamping, S.R., Zhang, H., Allen, B., Shamlou, P.A., 2003. Design of a prototype miniature bioreactor for high throughput automated bioprocessing. *Chem. Eng. Sci.* 58, 747–758.
- Lye, G.J., Ayazi-Shamlou, P., Baganz, F., Dalby, P.A., Woodley, J.M., 2003. Accelerated design of bioconversion process using automated microscale processing technique. *Trends Biotechnol.* 21 (1), 29–37.
- Maharbiz, M.M., Holtz, W.J., Howe, R.T., Keasling, J.D., 2004. Microbioreactor array with parametric control for high-throughput experimentation. *Biotechnol. Bioeng.* 85 (4), 376–381.
- Puskeiler, R., Kaufmann, K., Weuster-Botz, D., 2005. Development, parallelization, and automation of a gas-inducing milliliter-

- scale bioreactor for high-throughput bioprocess design (HTBD). *Biotechnol. Bioeng.* 89, 512–523.
- Rubinstein, L.J., Stein, K.E., 1988. Murine immune response to the *Neisseria meningitidis* group C capsular polysaccharide. II. Specificity. *J. Immunol.* 141 (12), 4357–4362.
- Tolosa, L., Kostov, Y., Harms, P., Rao, G., 2002. Noninvasive measurement of dissolved oxygen in shake flasks. *Biotechnol. Bioeng.* 80 (5), 594–597.
- Van Houten, K.A., Heath, D.C., Barringer, C.A., Rheingold, A.L., Pilato, R.S., 1998. Functionalized 2-pyridyl-substituted metallo-1,2-enedithiolates. Synthesis, characterization, and photophysical properties of $(dppe)M\{S_2C_2(CH_2CH_2OR'')\}$ and $(dppe)M[\{S_2C_2(CH_2CH_2-N-2-pyridinium)\}]^+$ ($R''=H, acetyl, lauroyl$; $M=Pd, Pt$; $dppe=1,2-bis(diphenylphosphino)ethane$). *Inorg. Chem.* 37, 4647.
- Weuster-Botz, D., Puskeiler, R., Kusterer, A., Kaufmann, K., John, G.T., Arnold, M., 2005. Methods and milliliter-scale device for high-throughput bioprocess design. *Bioprocess. Biosyst. Eng.* 28 (2), 109–119.
- Wright, G.W., Simon, R.M., 2003. A random variance model for detection of differential gene expression in small microarray experiments. *Bioinformatics* 19 (18), 2448–2455.
- Yang, Y.H., Dudoit, S., et al., 2002. Normalization for cDNA microarray data: a robust composite method addressing single and multiple slide systematic variation. *Nucleic Acids Res.* 30 (4), e15.
- Zanzotto, A., Boccazzi, P., Gorret, N., Van Dyk, T.K., Sinskey, A.J., Jensen, K.F., 2005. In situ measurement of bioluminescence and fluorescence in an integrated microbioreactor. *Biotechnol. Bioeng.* 93 (1), 40–47.
- Zanzotto, A., Szita, N., Boccazzi, P., Lessard, P., Sinskey, A.J., Jensen, K.F., 2004. Membrane-aerated microbioreactor for high-throughput bioprocessing. *Biotechnol. Bioeng.* 87 (2), 243–254.